# What Caused the Significant Increase in Atlantic Ocean Heat Content Since the mid-20th Century?

Sang-Ki Lee[1,2], Wonsun Park[3], Erik van Sebille[5], Molly Baringer[2], Chunzai Wang[2], David B. Enfield[1,2], Steven Yeager[4], and Ben Kirtman[5]

[1]Cooperative Institute for Marine and Atmospheric Studies, University of Miami, Miami, Florida, USA

[2]Atlantic Oceanographic and Meteorological Laboratory, NOAA, Miami Florida, USA

[3]Leibniz Institute of Marine Sciences (IFM-GEOMAR), Kiel, Germany

[4]National Center for Atmospheric Research, Boulder, Colorado, USA

[5]Rosenstiel School for Marine and Atmospheric Science, University of Miami, Miami, Florida, USA

Submitted to Geophysical Research Letters

May 2011

Corresponding author address: Dr. Sang-Ki Lee, NOAA/AOML, 4301 Rickenbacker Causeway, Miami, FL 33149, USA. E-mail: Sang-Ki.Lee@noaa.gov.

**Abstract**

As the upper layer of the world ocean warms gradually during the 20th century, the inter-ocean heat transport from the Indian to Atlantic basin should be enhanced, and the Atlantic Ocean should therefore gain extra heat coming the Indian Ocean. Consistent with this hypothesis, instrumental records indicate that the Atlantic Ocean has warmed substantially more than any other ocean basin since the mid-20th century. A surface-forced global ocean-ice coupled model is used to test this hypothesis and to further find that the increased wind stress curl since the 1950s over the South Atlantic and Indian subtropical gyres has contributed greatly to the increased inter-ocean heat transport from the Indian Ocean via increased Agulhas Current leakage.

## 1. Introduction

Recently updated and bias-corrected instrumental records indicate that the heat content of the Atlantic Ocean in the upper 700 m has substantially increased during the 1970s – 2000s at a rate (~ $2.0\times10^{22}$ J per decade) almost matching that of the Pacific Ocean (~ $1.5\times10^{22}$ J per decade) and Indian Ocean (~ $0.5\times10^{22}$ J per decade) combined [Levitus et al., 2009], even though the Atlantic Ocean covers less than 20% of the global ocean in surface area. Climate model experiments with and without anthropogenic greenhouse forcing have shown that the observed warming of the global ocean since the mid-20th century could be largely attributed to the anthropogenic greenhouse effect [e.g., Levitus et al., 2001]. However, a question still remains as to why the warming trend in the Atlantic Ocean is substantially larger than that in other ocean basins. This is also an important question for our understanding of past, present and future climate variability on regional and global scales. For example, recent studies have shown that tropical precipitation and Atlantic hurricane activity in the 21st century could be affected by a differential inter-ocean warming [e.g., Xie et al., 2010; Lee et al., 2011].

Levitus et al. [2000] argued that deep convective mixing over the North Atlantic sinking regions could maintain the subpolar North Atlantic sea surface temperatures (SSTs) relatively insensitive to the anthropogenic greenhouse effect, and thus decreasing the longwave heat loss at the sea surface and increasing the radiative heating associated with anthropogenic greenhouse gases (back radiation – upward longwave radiation). However, this hypothesis appears to be inconsistent with the observed cooling trend of the subpolar North Atlantic Ocean in the upper 1500 m during the 1950s - 1990s [e.g., Lozier et al. 2010].

Perhaps, the answer to this conundrum can be found in the global overturning circulation, that is large scale ocean circulation that connects the Pacific, Indian and Southern Oceans to deep

convection in the North Atlantic sinking regions, carrying with it heat, freshwater and carbon, etc [Broecker, 1987]. As the upper layer of the world ocean warms gradually, the inter-ocean heat transport via the global overturning circulation should increase given that the radiative heating associated with the anthropogenic greenhouse effect is more or less uniform over the world ocean. The increased inter-ocean heat transport should further warm the Atlantic Ocean since the Atlantic basin is characterized with advective heat convergence (i.e., the northward ocean heat transport at $30^{o}$S in the South Atlantic is always positive) due to the Atlantic Meridional Overturning Circulation (AMOC), which is the Atlantic component of the global overturning circulation. The Atlantic warming should continue until the deep layer of the Atlantic Ocean fully adjusts to the increased radiative heating over the world ocean and exports the warm water out of the basin at depth or until the AMOC weakens due to the increased buoyancy in the North Atlantic sinking regions.

The observed warming trend during the latter half of the 20th century is large in both North and South Atlantic basins [Levitus et al., 2000; 2009]. This suggests anomalous advective heat convergence in both the South and North Atlantic basins, and hence a larger increase in the ocean heat transport into the South Atlantic at $30^{o}$S and a lesser increase into the North Atlantic. Obviously, this suggests that the strength and spatial structure of the AMOC may have shifted since the mid-20th century. However, it is difficult to attribute the increased Atlantic Ocean heat content to AMOC variability because there is no reliable long-term instrumental record of the AMOC. It appears that an ocean model-based reconstruction is likely to be our best chance for assessing the history of AMOC in the 20th century thanks to the relatively long time series available for the observed surface flux fields, which constrain ocean-only (or ocean-ice coupled) models. Therefore, in the following sections, we use a series of global ocean-ice model

simulations to explore why the Atlantic Ocean has warmed much more than any other ocean basin since the mid-20th century.

## 2. 20th Century Reanalysis (20CR)

It is virtually impossible to properly initialize a global ocean model at the mid-20th century due to the paucity of observational hydrographic data during that period. An alternative approach is to start an ocean model simulation sufficiently earlier than the mid-20th century with an arbitrary set of initial conditions. However, none of the surface-forced ocean model studies so far has been simulated with the surface forcing prior to the mid-20th century because the surface forcing data, which are typically derived from atmospheric reanalysis products such as NCEP-NCAR reanalysis, are limited to the last 50 - 60 years. Recently, the newly developed NOAA-CIRES 20th Century Reanalysis (20CR) has been completed [Compo et al., 2010]. The 20CR provides the first estimate of global surface momentum, heat and freshwater fluxes spanning the late 19th century and the entire 20th century (1871-2008) at daily temporal and $2^{o}$ spatial resolutions.

## 3. Model Experiments

The global ocean-ice coupled model of the NCAR Community Climate System Model version 3 (CCSM3) forced with the 20CR is used as the primary tool in this study. The ocean model is a level-coordinate model based on the Parallel Ocean Program (POP). It solves the three-dimensional primitive equations under hydrostatic and Boussinesq approximations. The ocean model is divided into 40 vertical levels. The ice model, the NCAR Community Sea Ice Model version 5, is a dynamic-thermodynamic ice model that computes local growth rates of sea

ice due to vertical conductive, radiative and turbulent fluxes. Both the ocean and ice models have 320 longitudes and 384 latitudes on a displaced pole grid with a longitudinal resolution of about 1.0 degrees and a variable latitudinal resolution of approximately 0.3 degrees near the equator. See Doney et al. (2007) for more detailed descriptions about the CCSM3 ocean-ice model (CCSM3_POP hereafter).

To spin up the model, the fully coupled (atmosphere-land-ocean-ice) CCSM3 control experiment is performed for 700 years with the pre-industrial climate condition of the 1870s. The 700th year output of the CCSM3 spin-up run is then used to initialize the CCSM3_POP, which is further integrated for 200 more years using the daily 20CR surface flux fields for the period of 1871-1900. To incorporate the impact of atmospheric noise, which plays a crucial role in the thermohaline convection and deep-water formation in the North Atlantic sinking regions, during the spin-up the surface forcing fields in each model year are alternated with those of a randomly selected year from 1871 to 1900. In the 200 years of the CCSM3_POP spin-up run, the simulated world ocean heat content in the upper 700m shows no sign of drift after about 150 years. Nevertheless, the 900 years of spin-up may not be long enough for deep oceans to reach a quasi-equilibrium state, if there is any. Therefore, to check and ensure that there is no long-term model drift in the real-time experiments to be described below, the CCSM3_POP spin-up run is continued for additional 138 years, which is referred to as the reference experiment (EXP_REF).

After the total of 900 years of spin up runs, three model experiments are performed as summarized in Table 1. In the control experiment (EXP_CTR), the CCSM3_POP is integrated for 1871-2008 using the real-time daily 20CR surface flux fields. The next two experiments are idealized experiments designed to understand the Atlantic Ocean heat content change with and without the influence of the northward heat transport change at $30^{o}$S. The remote ocean warming

experiment (EXP_REM) is identical to EXP_CTR except that the surface forcing fields north of 30$^{o}$S are from the daily 20CR surface flux fields for the period of 1871-1900 exactly like the spin-up experiment, whereas those south of 30$^{o}$S are real time as in EXP_CTR. The Atlantic Ocean warming experiment (EXP_ATL) is also identical to EXP_CTR except that the surface forcing fields south of 30$^{o}$S are from the daily 20CR surface flux fields for the period of 1871-1900 as in the spin-up experiment, whereas those north of 30$^{o}$S are real time as in EXP_CTR. Note that the Atlantic Ocean warms only through anomalous surface warming in EXP_ATL, and only through anomalous northward ocean heat transport at 30$^{o}$S in EXP_REM, respectively.

## 4. Results

Figure 1a shows the time series of simulated Atlantic Ocean heat content in the upper 700m in reference to the 1871-1900 baseline period obtained from the three model experiments, along with the observed trend of the Atlantic Ocean heat content. The observed trend is referenced in 1969 for a better visual comparison with the simulated trends. The simulated heat content of the Atlantic Ocean in EXP_CTR increases moderately during the first half of the 20th century, after which it increases substantially. During the 1970s – 2000s, it increases by 5 ~ 6×10$^{22}$ J. This large increase is reasonably close to the observed Atlantic Ocean heat content increase of 7 ~ 8×10$^{22}$ J during the same period [Levitus et al., 2009], suggesting that the model experiment (EXP_CTR) reproduces reasonably well the heat budget trend of the Atlantic Ocean after the 1960s. If the northward heat transport in the South Atlantic at 30$^{o}$S is fixed at its 1871-1900 level (EXP_ATL), the North Atlantic Ocean heat content increases by only ~ 2×10$^{22}$ J during the 1970s - 2000s; thus the local variable surface fluxes alone cannot explain the observed North Atlantic Ocean heat content increase. On the other hand, if the northward heat transport in the

South Atlantic at 30$^{o}$S is allowed to vary in real time while keeping the surface fluxes over the Atlantic Ocean at their 1871-1900 levels (EXP_REM), the Atlantic Ocean heat content increases by 3 ~ 4×10$^{22}$ J during the 1970s – 2000s explaining a large portion of the simulated trend in EXP_CTR. The simulated Atlantic Ocean heat content in EXP_REF does not show any long-term model drift affirming that the increased Atlantic Ocean heat content in EXP_CTR is not an artifact of the model simulation.

Figure 1b shows the heat budget terms for the Atlantic Ocean, obtained from EXP_CTR, namely the northward heat transport for the entire water column at 30$^{o}$S, the surface heat flux into the Atlantic Ocean between 30$^{o}$S and 75$^{o}$N, and the northward heat transport for the entire water column at 75$^{o}$N multiplied with –1, all referenced to the 1871-1900 baseline period. The simulated northward heat transport at 30$^{o}$S is about 0.1 ~ 0.2 PW larger in the 1960s - 2000s period than in the earlier periods, consistent with the large Atlantic Ocean heat content increase in EXP_CTR (Figure 1a). On the other hand, it is clear that both the surface heat flux and the northward Atlantic Ocean heat transport at 75$^{o}$N have little impact on the Atlantic Ocean warming since the mid-20th century. Therefore, these model results fully support the hypothesis that the enhanced warming of the Atlantic Ocean during the latter half of the 20th century is largely due to the increased ocean heat transport into the Atlantic basin across 30$^{o}$S.

## 5. AMOC Variability at 30$^{o}$S

Dong et al. [2009] showed that the northward heat transport in the South Atlantic near 30°S can be directly scaled with the AMOC strength. Therefore, the baroclinic volume transport (i.e., AMOC) in the South Atlantic at 30$^{o}$S and its contribution to the large increase (0.1 ~ 0.2 PW) in the simulated ocean heat transport into the Atlantic basin is explored in this section.

Figure 2a shows the time-averaged AMOC during 1979-2008 obtained from EXP_CTR. The simulated maximum strength of the AMOC at 35$^{o}$N is only 11 Sv (1Sv = $10^6$ $m^3s^{-1}$), which is smaller than the observed range of 14 ~ 20Sv. Increasing the vertical diffusivity in the model boosts the AMOC strength as shown in earlier studies. However, since other model features deteriorate with the increased vertical diffusivity, the vertical diffusivity is not increased in this study. Despite the smaller maximum strength, the overall spatial structure of the simulated AMOC is quite close to that derived from observations [e.g., Lumpkin and Spear 2007].

Figure 2b shows the time series of the simulated AMOC index (maximum overturning streamfunction) at 30$^{o}$S. It clearly shows that the AMOC at 30$^{o}$S increases after the 1940s, suggesting that the increased northward heat transport in the South Atlantic at 30$^{o}$S (Figure 1b) is linked to the increased baroclinic volume transport at 30$^{o}$S. The AMOC at 30$^{o}$S in EXP_REM has a similar increase as in EXP_CTR (Figure S1a). On the other hand, the AMOC at 30$^{o}$S in EXP_ATL (Figure S1b) does not show a large long-term trend. These results strongly suggest that the processes within the Atlantic Ocean do not cause the increased AMOC strength at 30oS after the 1940s in EXP_CTR. In other words, the AMOC increase at 30$^{o}$S is pushed from the outside, and not pulled from the inside.

The effect of the increased AMOC versus the increased upper ocean temperature in the South Atlantic at 30°S can be assessed by using the model output fields from EXP_CTR. Using only the Eulerian-mean component of the meridional flow (i.e., eddy-induced component is not used) and the ocean temperature, we find that the purely thermal effect (i.e., only due to ocean temperature changes) accounts for about 20% increase of the heat transport at 30$^{o}$S between 1871-1900 and 1979-2008 periods, whereas the purely dynamic effect (i.e., only due to meridional flow changes) accounts for more than 120% increase, clearly suggesting that the

upper ocean thermal change of the inflow is insufficient to explain the large increase (0.1 ~ 0.2 PW) in the simulated ocean heat transport into the Atlantic basin.

## 6. The Role of South Atlantic and Indian Subtropical Gyres

The main conclusion so far is that the observed large warming of the Atlantic basin during the latter half of the 20th century is mainly due to the increased ocean heat transport into the Atlantic basin across $30^{o}$S, and that the anomalous northward ocean heat transport at $30^{o}$S is caused not only by the increased upper ocean temperature at $30^{o}$S but also and more strongly by the increased baroclinic volume transport (i.e., AMOC) at $30^{o}$S.

Remote mechanical and thermal forcing appear to strengthen the AMOC and associated heat transport at 30°S. In order to understand the mechanisms, it is helpful to explore the simulated pathways of the northward heat transport in the Atlantic Ocean. Shown in Figure 3a are the simulated northward heat transport (contours) and heat transport vector (vectors) averaged in the upper 3000m for 1979-2008, obtained from EXP_CTR. It clearly shows that the main pathway of heat into the South Atlantic in this model originates in the Indian Ocean. The key roles played in global climate by the Indian-Atlantic inter-ocean exchange have long been recognized [e.g., Biastoch et al., 2008; Beal et al. 2011]. The warm water that leaks from the Indian Ocean, the so-called Agulhas leakage, into the South Atlantic may affect the strength of the AMOC, both on decadal advective time scales and on faster Rossby wave time scales [e.g., Van Sebille and Van Leeuwen, 2007]. As shown in Figure 3a, the warm water entrained from the Indian Ocean moves northwestward along the South Atlantic subtropical gyre until it reaches the western boundary, then continues its northward excursion through the cross-hemispheric western boundary current system. The warm water finally arrives at the subpolar Atlantic via the Loop Current, Gulf

Stream and North Atlantic Current, respectively. The pathways of the heat transport shown in Figure 3a are very similar to the advective pathways of mass seen in both high-resolution models and surface drifters [Van Sebille et al., 2011].

Figure 3b is identical to Figure 3a except that it shows the difference in the simulated northward heat transport (contours) and heat transport vector (vectors) between 1979-2008 and 1871-1900 periods. The pathways of the anomalous northward ocean heat transport are surprisingly similar to those of the mean northward ocean heat transport (Figure 3a). It is also clear that the inter-ocean heat transport from the Indian Ocean is increased. This agrees with observations in the Agulhas region, on the boundary between the Indian and Atlantic Oceans, which show an increase in both upper ocean temperature [Rouault et al., 2009] and inter-ocean transport [Biastoch et al., 2009] in recent decades. The anomalous anticyclones of the barotropic stream function in the South Atlantic and Indian Ocean between $50^{o}$S and $30^{o}$S (Figure S2) further indicate that both the South Atlantic subtropical gyre and Indian Ocean subtropical gyre are strengthened. As shown in Figure 3c, this is consistent with the observed westerly wind anomalies over the Southern Ocean and the associated strengthening of the wind stress curl over the South Atlantic and Indian subtropical gyres, as suggested by earlier high- and low-resolution modeling studies [Biastoch et al., 2009; Sijp and England, 2009]. It is important to note that Ekman transport does not directly contribute to the increased AMOC at $30^{o}$S since the zonal wind stress at $30^{o}$S is nearly unchanged (Figure 3c). Since the westerly wind anomalies over the Southern Ocean are largely linked to the Southern Annular Mode (SAM), it appears that the increased AMOC at $30^{o}$S in EXP_CTR is ultimately caused by the increasing trend of the SAM since the mid-20th century. The cause of the SAM trend is not the focus of this study, but one

popular hypothesis involves the Antarctic ozone losses with important contributions from anthropogenic chlorofluorocarbons [e.g., Thompson and Solomon, 2002].

## 7. Discussions

This study uses a series of global ocean-ice model simulations, which are forced with the newly constructed 20CR for the period of 1871-2008, to argue that the observed warming trend of the Atlantic Ocean during the latter half of the 20th century is largely due to the concurrent increase of the northward ocean heat transport in the South Atlantic at 30$^{o}$S. It is shown here that the anomalous northward ocean heat transport at 30$^{o}$S is caused by the increased inter-ocean heat transport from the Indian Ocean. In agreement with earlier studies, the increased inter-ocean heat transport is augmented by the strengthening of the wind stress curl since the mid-20th century over the South Atlantic and Indian subtropical gyres in association with the observed increasing trend of the SAM.

There are some limitations in this study. In particular, the CCSM3_POP used as the main tool in this study is not an eddy-resolving resolution model. Therefore, it is important that the major findings of this study are further tested with higher resolution models. In particular, eddy-resolving resolution (~ 0.1 deg) models are required to properly simulate the role of eddies in the Agulhas leakage region. A related issue is the eddy-driven heat and mass transports in the Southern Ocean, which are not well represented in this study [e.g., Hallberg and Gnanadesikan, 2006]. Nevertheless, a recent study that uses an eddy-resolving model reported an increased volume transport from the Indian Ocean to the South Atlantic Ocean during the 1970s – 2000s [Biastoch et al., 2009], supporting the overall conclusions of this study.

Obviously, there remain many crucial questions. One such question is the contribution of the Atlantic Multidecadal Oscillation (AMO), which is arguably resulted from the natural oscillation of the AMOC and driven in the North Atlantic sinking regions [e.g., Knight et al. 2005; Lee and Wang, 2010], in the rapid warming of the Atlantic Ocean since the 1950s. Another related question is whether the increased buoyancy in the North Atlantic Ocean will eventually lead to decreased North Atlantic deep convection in the 21st century. These are only examples of many questions to be addressed in the future work.

**Acknowledgments.** This study was motivated and benefited from the AMOC discussion group of the research community at UM/RSMAS and NOAA/AOML. We wish to thank Igor Kamenkovich and all the participants who led the AMOC discussion group during the past year. We acknowledge helpful suggestions from Ping Chang. This work was supported by grants from the National Oceanic and Atmospheric Administration's Climate Program Office and by grants from the National Science Foundation.

## References

Beal, L. M., W. P. M. De Ruijter, A. Biastoch, R. Zahn, and members of SCOR/ WCRP/IAPSO Working Group 136 (2011) On the role of the Agulhas system in ocean circulation and climate, **Nature**, 472, doi:10.1038/nature09983, 429-472.

Biastoch, A., C. W. Boening, and J. R. E. Lutjeharms (2008) Agulhas leakage dynamics affects decadal variability in Atlantic overturning circulation, Nature, **456**, 489–492.

Biastoch, A., C. W. Böning, F. U. Schwarzkopf, and J. R. E. Lutjeharms (2009) Increase in Agulhas leakage due to poleward shift in the southern hemisphere westerlies, *Nature*, **462**, doi:10.1038/nature08519, 495-498.

Broecker, W. S. (1987) The biggest chill, *Natural History*, **96**, 74-82.

Compo, G. P., and collaborators (2011) The twentieth century reanalysis project. *Quarterly J. Roy. Meteorol. Soc*., **137**, 1-28. doi: 10.1002/qj.776.

Doney, S. C., Steve Yeager, G. Danabasoglu, W. G. Large, J. C. McWilliams (2007) Mechanisms governing interannual variability of upper-ocean temperature in a global ocean hindcast simulation. *J. Phys. Oceanogr*., **37**, 1918–1938.

Dong, S., S. L. Garzoli, M. O. Baringer, C. S. Meinen and G. J. Goni (2009) Interannual variations in the Atlantic meridional overturning circulation and its relationship with the net northward heat transport in the South Atlantic. *Geophys. Res. Let*t., **36**, L20606, doi:10.1029/2009GL039356.

Hallberg, R.W. and A. Gnanadesikan (2006) The role of eddies in determining the structure and response of the wind-driven Southern Hemisphere overturning: Initial results from the Modeling Eddies in the Southern Ocean Project, *J. Phys. Oceanogr*., **36**, 2232-2252.

Knight, J. R., R. J. Allan, C. K. Folland, M. Vellinga, and M. E. Mann (2005) A signature of persistent natural thermohaline circulation cycles in observed climate, *Geophys. Res. Let*t., 32, L20708, doi:10.1029/2005GL024233.

Lee, S.-K. and C. Wang (2010). Delayed advective oscillation of the Atlantic thermohaline circulation. *J. Climate*, **23**, 1254-1261.

Lee, S.-K., D. B. Enfield and C. Wang (2011) Future impact of differential inter-basin ocean warming on Atlantic hurricanes. *J. Climate*, in-press.

Levitus, S., J. I. Antonov, T. P. Boyer, and C. Stephens (2000) Warming of the world ocean. *Science* **287**, 2225-2229, doi:10.1126/science.287.5461.2225.

Levitus, S., J. I. Antonov, J. Wang, T. L. Delworth, K. W. Dixon, and A. J. Broccoli (2001) Anthropogenic warming of earth's climate system, *Science* **287**, 2225-2229, doi:10.1126/science.287.5461.2225.

Levitus, S., J. I. Antonov, T. P. Boyer, R. A. Locarnini, H. E. Garcia, and A. V. Mishonov (2009) Global ocean heat content 1955–2008 in light of recently revealed instrumentation problems, *Geophys. Res. Lett*., **36**, L07608, doi:10.1029/2008GL037155.

Lozier, M. S., V. Roussenov, S. Mark, C. Reed and R. G. Williams (2010) Opposing decadal changes for the North Atlantic meridional overturning circulation. *Nature Geosci*. **3**, 728-734.

Lumpkin, R. and K. Speer (2007) Global ocean meridional overturning. *J. Phys. Oceanogr.*, **37**, 2550-2562.

Rouault, M., P. Penven, and B. Pohl (2009), Warming in the Agulhas Current system since the 1980's, *Geophys. Res. Lett*., **36**, L12, 602.

Sijp, W. P., and M. H. England (2009) Southern hemisphere westerly wind control over the ocean's thermohaline circulation. *J. Climate*, **22**, 1277-1286.

Thompson, D. W. and S. Solomon (2002) Interpretation of recent southern hemisphere climate change, 296, 895-899, doi:10.1126/science.1069270.

Van Sebille, E., and P. J. Van Leeuwen (2007) Fast northward energy transfer in the Atlantic due to Agulhas rings, *J. Phys. Oceanogr*., 37, 2305–2315.

Van Sebille, E., L. M. Beal, and W. E. Johns (2011) Advective time scales of Agulhas leakage to the North Atlantic in surface drifter observations and the 3D OFES model, *J. Phys. Oceanogr.*, in press.

Xie, S.-P., C. Deser, G.A. Vecchi, J. Ma, H. Teng, and A.T. Wittenberg (2010) Global warming pattern formation: Sea surface temperature and rainfall. *J. Climate*, 23, 966-986.

Table 1. Summary of the surface forcing fields prescribed for the four model experiments.

| Experiments | Surface Forcing Fields Prescribed |
|---|---|
| EXP_REF | Forced for 138 years with the forcing fields in each model year alternated with the 20CR forcing fields of a random year during 1871 - 1900. |
| EXP_CTR | Forced for 1871-2008 using the real-time 20CR. |
| EXP_REM | Same as in EXP_CTR south of 30$^{o}$S; Same as in EXP_REF north of 30$^{o}$S |
| EXP_ATL | Same as in EXP_REF south of 30$^{o}$S; Same as in EXP_CTR north of 30$^{o}$S |

**Figure 1**. (a) Simulated Atlantic Ocean heat content change in the upper 700m in reference to the 1871-1900 baseline period obtained from the four model experiments. The thick black line in (a) is the observed trend of the Atlantic Ocean heat content. (b) Simulated heat budget terms for the Atlantic Ocean obtained from EXP_CTR, all referenced to the 1871-1900 period.

**Figure 2.** (a) Time-averaged AMOC during 1979-2008 and (b) time series of the simulated AMOC index (maximum overturning streamfunction) at $30^{o}$S obtained from EXP_CTR. The green line in (b) is obtained by performing a 11- year running average to the AMOC index.

**Figure 3**. (a) Simulated pathways of the northward heat transport (contours) and heat transport vector (vectors) in the upper 3000 m for 1979-2008 obtained from EXP_CTR. The unit is $1\times10^{9}$ W/m. (b) Differences in the simulated northward heat transport (contours) and heat transport vector (vectors) between 1979-2008 and 1871-1900 periods, obtained from EXP_CTR. Red color indicates northward heat transport, while blue color indicates southward heat transport. (c) Globally averaged zonal wind stress for 1871-1900 and for 1979-2008 periods, obtained from the 20CR.

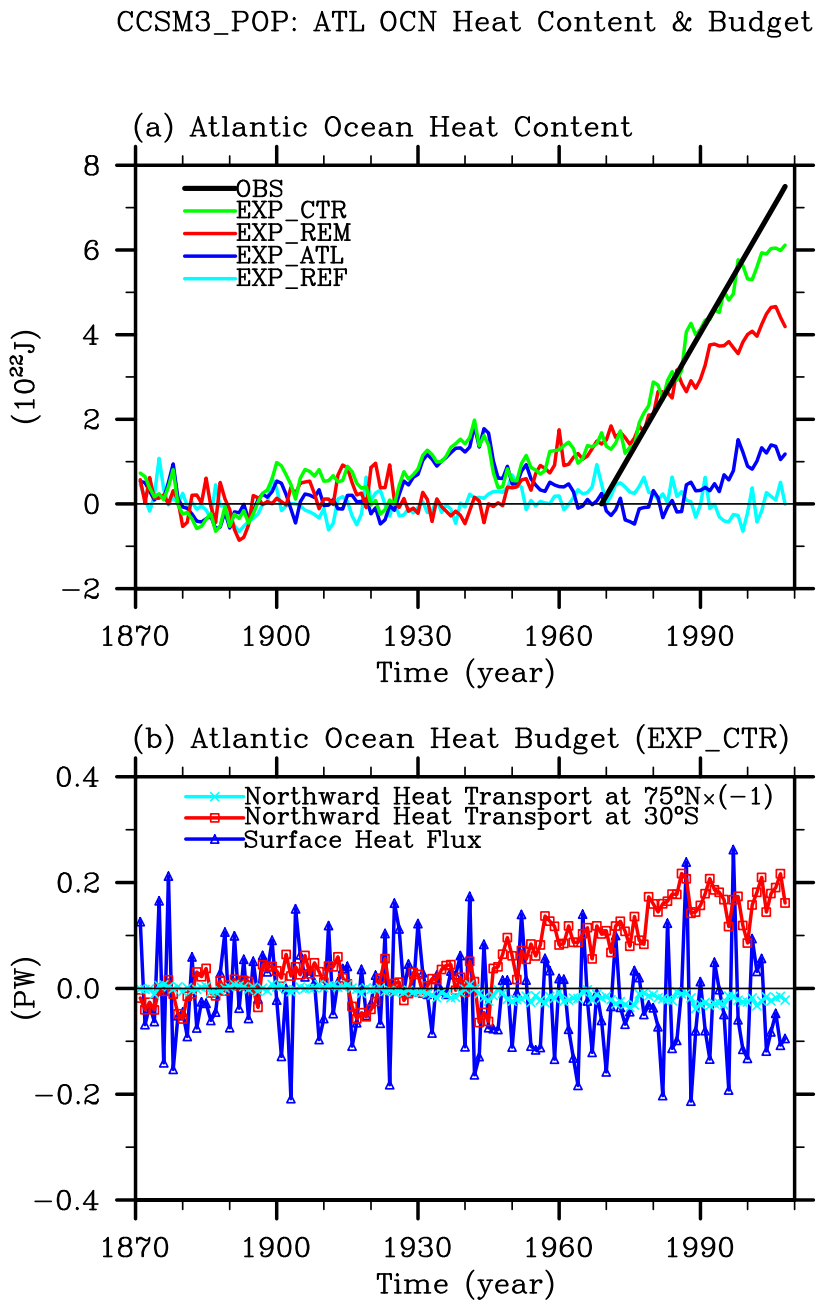


**Figure 1**. (a) Simulated Atlantic Ocean heat content change in the upper 700m in reference to the 1871-1900 baseline period obtained from the four model experiments. The thick black line in (a) is the observed trend of the Atlantic Ocean heat content. (b) Simulated heat budget terms for the Atlantic Ocean obtained from EXP_CTR, all referenced to the 1871-1900 baseline period.

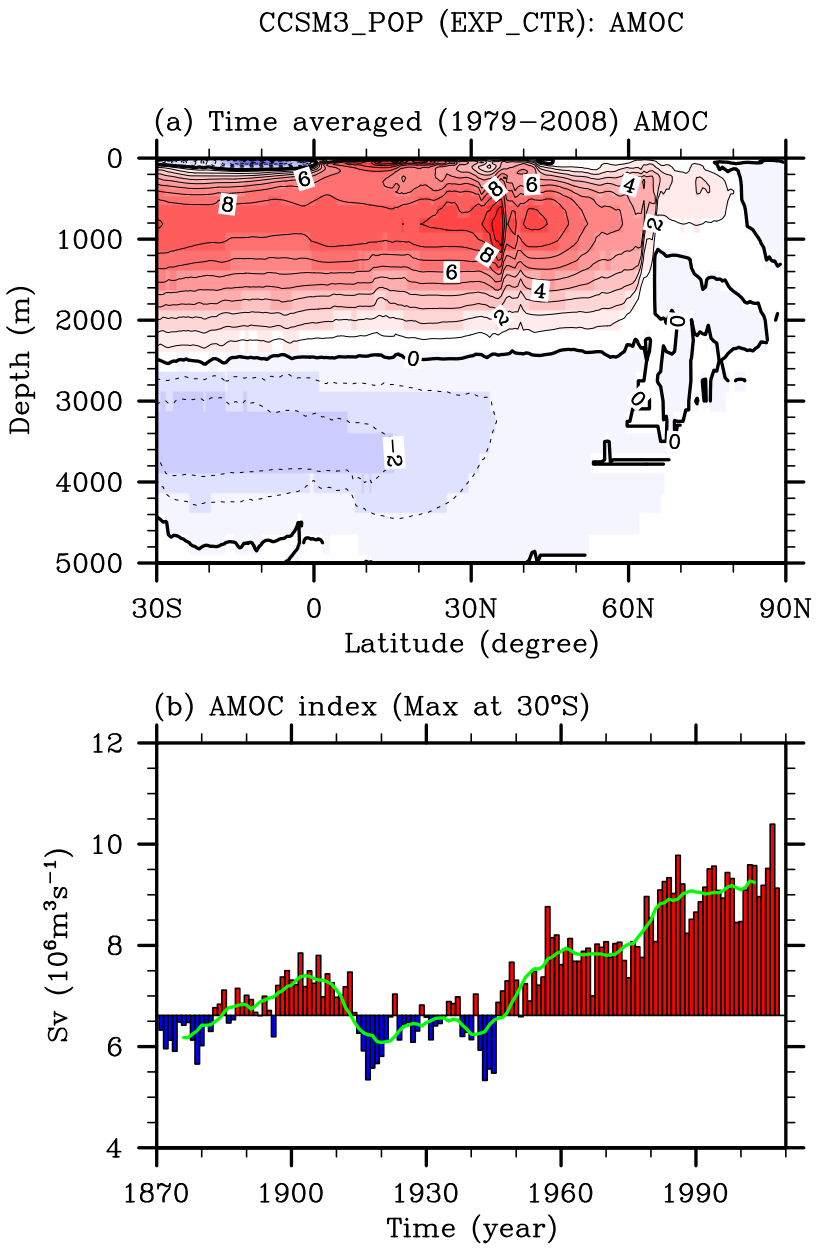


**Figure 2.** (a) Time-averaged AMOC during 1979-2008 and (b) time series of the simulated AMOC index (maximum overturning streamfunction) at 30$^{o}$S obtained from EXP_CTR. The green line in (b) is obtained by performing a 11- year running average to the AMOC index.

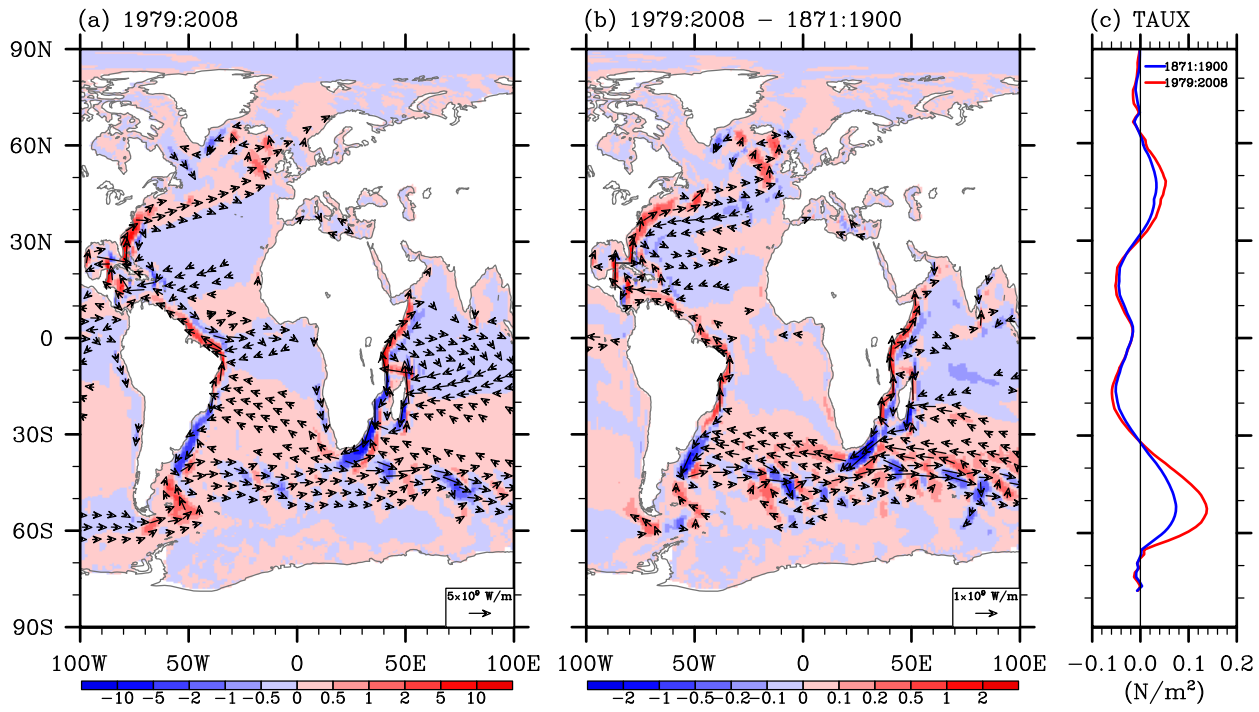


**Figure 3**. (a) Simulated pathways of the northward heat transport (contours) and heat transport vector (vectors) in the upper 3000 m for 1979-2008 obtained from EXP_CTR. The unit is $1\times10^9$ W/m. (b) Differences in the simulated northward heat transport (contours) and heat transport vector (vectors) between 1979-2008 and 1871-1900 periods, obtained from EXP_CTR. Red color indicates northward heat transport, while blue color indicates southward heat transport. (c) Globally averaged zonal wind stress for 1871-1900 and for 1979-2008 periods, obtained from the 20CR.